

Comparing Blast Wave Propagation over a Porous Ground

Margaret Grace McKay

A capstone report submitted to the faculty of
Brigham Young University
In partial fulfillment of the requirements for the degree of

Bachelor of Science

Tracianne Neilsen, Advisor

Department of Physics and Astronomy

Brigham Young University

April 2022

Copyright © 2022 Margaret Grace McKay

All Rights Reserved

ABSTRACT

Comparing Blast Wave Propagation over a Porous Ground

Margaret Grace McKay

Department of Physics and Astronomy

Bachelor of Science

One way to monitor volcanoes is by recording their acoustic signals. These signals often have less background noise than seismic signals, which allows the acoustics to be more closely tied with volcanic events. To improve understanding of how to interpret signals from ballistic volcanic events, we recorded sound during two blast wave experiments, one with exploding balloons and the other with buried explosives. In both experiments, microphones were placed at varying distances and heights. The experiments were in different locations, and we had different resources and constraints, so the set-ups are similar but not the same. Comparisons of waveforms and spectra are made between the two different experiments. This comparison sheds some insights into blast wave propagation along and in a porous ground.

Keywords: volcano noise; shock wave; volcano acoustics; porous ground; seismo-acoustics

Acknowledgments

I want to thank the following organizations and people for their help and contributions to this project:

- Dr. Tracianne Neilsen in the Brigham Young University Physics Department for mentoring me through the entirety of this project
- My research group, Julio Escobedo, Carla Butts, Christian Lopez, Eric Lysenko, Sarah Ostergaard, and Menley Stewart
- BYU College of Physical and Mathematical Sciences Undergraduate Mentorship Program and the National Science Foundation (NSF-1757998) for funding undergraduate research assistants on this project
- University of Buffalo for sponsoring and hosting the 2018 Geohazards Workshop

Table of Contents

Table of Contents.....	v
List of Figures.....	vii
1 Introduction	2
1.1 Motivation.....	2
1.2 Background	3
1.3 Previous Research at BYU.....	5
1.4 Overview.....	7
2 Methods	8
2.1 Exploding Balloon Test	8
2.1.1 Background	8
2.1.2 Experiment.....	8
2.2 Geohazards Workshop Test.....	16
2.2.1 Background	16
2.2.2 Experiment.....	16
3 Results and Conclusions.....	20
3.1 Analysis Methods	20
3.2 Exploding Balloon Results.....	22
3.3 Geohazards Workshop	26
3.4 Conclusion	29

Appendix A	30
<i>Computer Codes.....</i>	<i>31</i>
<i>Specific Data Information</i>	<i>31</i>
<i>Weather Data – Kestrel.....</i>	<i>33</i>
Index.....	36
References.....	37

List of Figures

Figure 1-1 Acoustic wave paths of an elevated source and an in-ground source.	4
Figure 1-2 Models of the four different crater shapes used in the Exploding Balloons Experiment.	6
Figure 2-1 Examples of filling the gas filled balloons.	9
Figure 2-2 Oxyacetylene balloon held to the ground with Saran wrap to prevent popping and being blown away.	10
Figure 2-3 Infiniband cable box with eight channels plugged in.	11
Figure 2-4 A general diagram of the set-up of a microphone station.	14
Figure 2-5 Picture of the "Ground Mic".	14
Figure 2-6 Aerial view of the Exploding Balloons set-up.	15
Figure 2-7 Aerial view of the set-up at the University of Buffalo Geohazards Workshop.	18
Figure 2-8 Layout of the dynamite in the ground for each blast pad.	19
Figure 3-1 Example waveform from the Exploding Balloons Pretest.	20
Figure 3-2 Cutoff frequency of ground wave based on distance from source.	22
Figure 3-3 Waveform and Spectrogram of the microphone 100 m from the source and 1.2 m above the ground from the exploding balloons test.	23
Figure 3-4 Plot of the peak pressures of the Secondary Arrival wave as a function of their height.	24
Figure 3-5 Peak amplitudes of the secondary arrivals in the waveforms compared to geometric spreading as a function of distance.	25

Figure 3-6 Time aligned, normalized waveforms for “Pad 4” (in Figure 2-8) from the ground microphones at all distances.	27
Figure 3-7 The waveform and spectrogram for the ground microphone a distance of 230 m from the source.	28
Figure 3-8 Peak amplitudes of the secondary arrival compared to geometric spreading as a function of distance.	29
Figure 9 Normalized waveforms of the ground microphones during Pad 1 in the Geohazards Workshop stacked in order of distance.	32

1 Introduction

In this thesis I am comparing the acoustic shock waves from two separate experiments, the Exploding Balloons Pretest and the Geohazards Workshop. In these shock waves, we found evidence of ground waves in both experiments. Chapter 1 explains the previous research conducted and the goals of the experiments. Chapter 2 describes the experiments' set-up and procedures. Finally, Chapter 3 explains the analysis methods used, our results, and our conclusions. The results from this paper may assist in identifying the acoustic waves made from volcanic events.

1.1 Motivation

When volcanoes erupt, they emit both seismic and acoustic waves. The seismic waves cause the movement of the ground. Acoustic waves are the movement of air particles both above and in a porous ground. Volcanic events—such as large eruptions, small eruptions, and gas being released—produce seismic and acoustic waves that have unique signatures. These properties can be difficult to identify in seismic waves (because of other sources of seismic activity, like earthquakes) so the study of the acoustic waves can help identify volcanic events. An example of this is shown in Figure 3 of Robin Matoza's article "The Inaudible Rumble of Volcanic Eruptions" in the Spring 2018 issue of *Acoustics Today*¹.

A challenge in studying volcanoes is that there is often little forewarning of an eruption, resulting in little time to plan measurements of eruptions. Because of this difficulty, field experiments commonly use scaled explosions as models for real volcanic events². Similarly, the experiments discussed in this thesis are from scaled explosions. The first experiment, performed by Dr.

Neilsen's group used exploding balloons filled with oxyacetylene gas. The second experiment took place at the NSF-funded Geohazards Workshop at the University of Buffalo². A large collaboration of researcher worked together to measure many types of data from a series of buried explosives designed mimic the volcanic events.

1.2 Background

As sound propagates outdoors, the terrain effects how the sound wave travels. When sound from an elevated sound source travels over a solid hard surface, a direct sound wave arrives at the receiver and then a reflected sound wave follows shortly after. When modeling and analyzing acoustic waveforms, reflected waves³ needs to be accounted for. However, when sound travels over a porous ground like dirt, the sound interacts more with the ground; the ground absorbs a portion of the acoustic waves traveling through the air, as well as any reflected waves⁴. The absorbed energy can then be re-emitted as a type of ground wave.

In our own tests conducted over dirt, a secondary wave was evident that arrives after the initial blast wave. The placement of our sources on or in the ground also disprove any chance of this secondary wave being just a reflection. The secondary wave, also referred to as the secondary arrival, sometimes has a larger amplitude than the initial blast wave.

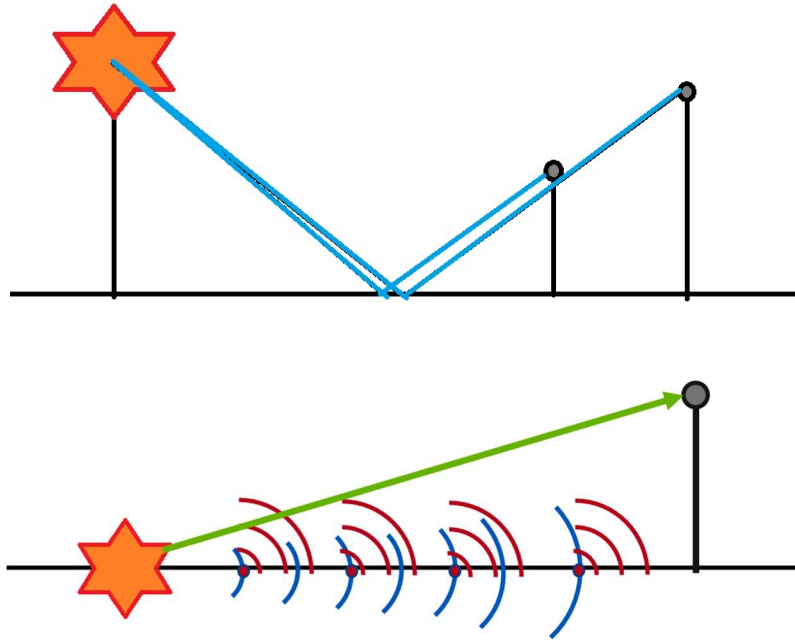


Figure 1-1 Acoustic wave paths of an elevated source and an in-ground source. The orange stars in both pictures represent the blast source. The top picture shows the reflected paths (in blue) from the elevated source to the two microphones (the gray circles). The bottom picture shows the direct path of the sound in green. There is another sound wave (shown in blue) that travels along the ground. Each part of the blue surface wave vibrates the ground which then acts as its own point source of sound shown as the red waves.

A key factor in our experiments is that our blast sources are on or in the ground. Most experiments, like those done previously at BYU, used an elevated source of sound^{3,5}. This source location provided a clear direct path for sound and a clear reflected path (seen in the top diagram of **Figure 1-1**). Our sources originate on or in the ground, so the reflected path is negligible. In our data we see the direct path but, as mentioned previously, we also see a low-frequency high-amplitude secondary wave that appears after the initial direct blast wave. With our sound source being on or in a porous ground, we know the acoustic wave not only travels through the air, but through the air inside the ground as well⁴. This in-ground vibration produces another acoustic

signal which arrives at the microphones after the initial blast wave. This phenomenon is shown in the bottom diagram of **Figure 1-1**.

1.3 Previous Research at BYU

Previously at BYU, Dr. Kent Gee's research group used exploding oxyacetylene balloons to study the nonlinear effects of acoustic shock propagation. Young *et al*³ analyzed the shock wave behavior with large balloons and long propagation distances. Leete *et al*⁵ focused on the nonlinear properties within a shorter propagation range of medium size exploding balloons and showed evidence of Mach stem formation. These previous experiments showed that oxyacetylene balloons have a large amplitude and powerful shock and, thus, should be a good blast source for our first experiment.

Dr. Neilsen's team consisted of six undergraduates and one middle-school teacher, Julio Escobar, who was participating in an NSF-funded Research Experience for Teachers (RET). The experiments have also been used for one Masters' Thesis (through the University of Utah's Masters in Secondary School Science Teaching program) and two other BYU undergraduate senior theses.

During his RET, Julio Escobedo studied the directionality of the acoustic shock waves based on the shape of the "crater" in which the balloon was placed. He wrote about this study in his Masters' Thesis⁶. The four different crater shapes, shown in **Figure 1-2**, contributed significantly to where the acoustic shock wave was directed. For my research project, I examine data from only one crater shape: Crater 1 in **Figure 1-2**.

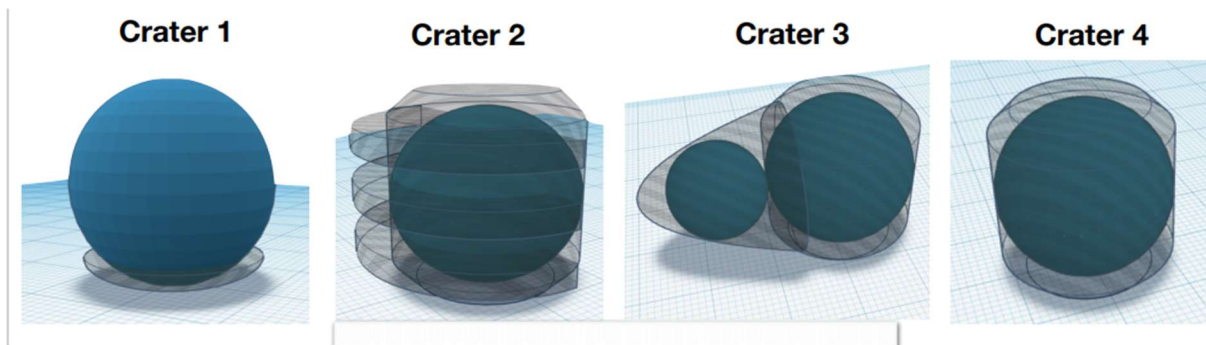


Figure 1-2 Models of the four different crater shapes used in the Exploding Balloons Experiment.

This thesis only focuses on Crater 1, but previous research done by Julio Escobedo focused on all four craters⁶.

In a BYU senior thesis, Sarah Ostergaard studied how to measure directionality when the exploding balloon was not in the center of a circle of microphones⁷. In the exploding balloon's test, we did trials on each crater with a full circle of microphones with the crater at the center and trials on each crater with a semi-circle of microphones centered on the point halfway between Crater 2 and Crater 3. This experimental layout is shown in **Figure 2-6**, with the yellow circles showing the general location of the circle microphone placements and the red circle showing the general placement of the semi-circle of microphones. Ostergaard used the data from the centered microphones and semi-circle microphones to try to figure out the true directionality of a source for when it's not placed in the center⁷.

As reported in another BYU senior thesis, Eric Lysenko measured the seismo-acoustic coupling of the blast waves⁸. Lysenko constructed a special box designed to block air-borne acoustic waves and allow only the ground radiated acoustic waves through to the microphone inside. The design of the box used materials that contributed to decoupling, absorption, and insulation. Using

both the field results and results from tests in the reverberation chamber on campus, he found that there was little detection of the coupled waves⁸.

1.4 Overview

The goal of this thesis is to analyze the secondary arrival wave that appears in our data from oxyacetylene balloon test and determine if it comes from a ground wave. We then use those same methods to prove the existence of ground waves in the Geohazards workshop. We base our methods of proof on the Embleton's "Outdoor Acoustics Tutorial," which is commonly used as a reference for outdoor acoustic experiments⁴. An understanding of the ground wave is important to correctly model and analyze sound waves generated over or in porous ground. More experiments like ours will contribute to better understanding acoustic signature from explosive volcanic events.

2 Methods

This chapter explains the methods used at both the exploding balloon test and the Geohazards workshop. The exploding balloon test, which was conducted in a field in Provo, Utah is described, followed by the Geohazards workshop test done in Buffalo, New York. The background of the tests, the equipment, layout, and procedures are discussed.

2.1 Exploding Balloon Test

2.1.1 Background

We set up a pretest with exploding balloons to prepare for the Geohazards Workshop in Buffalo. At the Geohazards workshop there were four explosions, each one slightly different configuration and location. To ensure our equipment, set-up, Data Acquisition (DAQ), and procedures ran as smoothly as possible, we conducted our own preliminary experiment. This pretest gave us the opportunity to identify the effect of a smaller scaled explosion in/on a porous ground before analyzing the larger ones.

2.1.2 Experiment

To investigate the impact of a porous ground on shock waves, we performed an experiment in a farmer's grazing field in Provo, Utah. The source of the shock waves were balloons filled with oxyacetylene gas. These balloons were put on and in pre-dug holes, called craters, in the ground.

2.1.2.1 Equipment

To generate shock waves, latex balloons were filled with oxyacetylene gas, more commonly known as welder's gas. This gas is a stoichiometric mixture of oxygen and acetylene which, when ignited, rapidly expands into carbon dioxide and water. The rubber rings as seen in **Figure 2-1** are to keep the mixture of the gases consistent between results and with the stoichiometric mixture. The balloon sizes used had diameters of 14", 17", 27", and 36". (We first blew up the balloons to test for holes and anything that could cause them to pop prematurely.) Each balloon was filled with the acetylene gas until it was the size of the smaller of the two rings. Then the balloon was filled with oxygen gas until it was the size of the larger ring which. We were provided different sets of rings to keep the mixture consistent for the desired sizes.

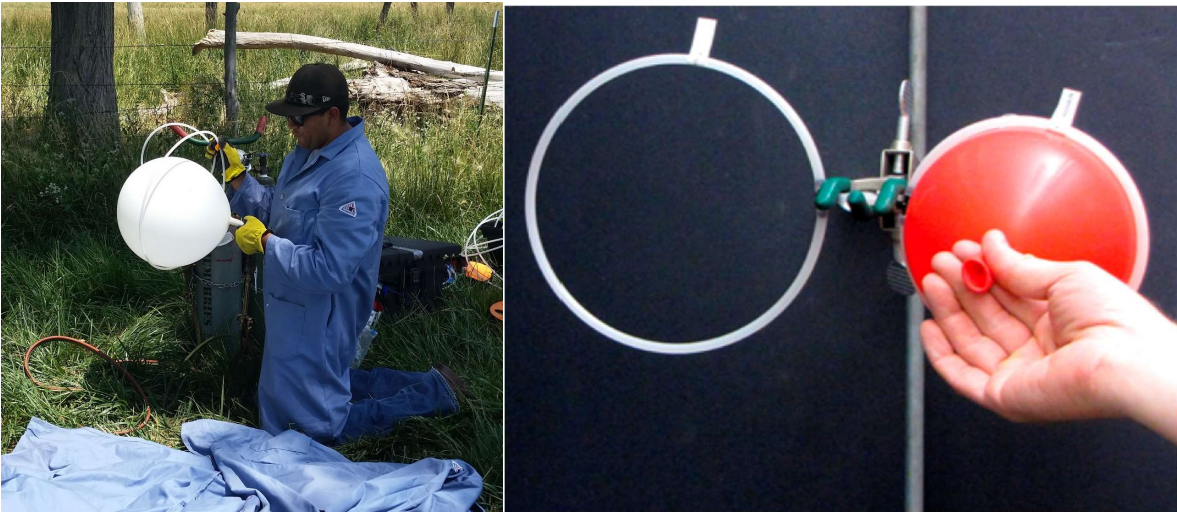


Figure 2-1 Examples of filling the gas filled balloons.

On the left, researcher Julio Escobedo using the rubber tubing to fill the balloons with an accurate stoichiometric mixture of oxygen and acetylene gas. On the right, an example of the different ring sizes used. These rings are smaller than the ones we used but their ratios are the same.

The balloons were held in place with Saran wrap, as shown in **Figure 2-2** and ignited from a model rocket ignitor. The crater was also lined with the Saran wrap to keep accidental popping to a minimum. The ignitor was connected via BNC cables and alligator clips to prevent accidental premature ignition.



Figure 2-2 Oxyacetylene balloon held to the ground with Saran wrap to prevent popping and being blown away.

This is the shallowest crater dug and the one that is analyzed in this thesis.

This experiment used two different kinds of microphones. The microphones used in the circle and semicircle (in **Figure 2-6**), were ¼” GRAS 40BE pre-polarized, free-field microphones.

These microphones have a frequency range from 10 Hz to 40 kHz at ± 1 dB and 4 Hz to 80 kHz at ± 2 dB. The microphones on the line array (located at the short, white vertical lines in **Figure 2-6**) were the ½” GRAS 40AE and 40AO pre-polarized microphones which have a frequency range of 5 Hz to 10 kHz at ± 1 dB and 3.15 Hz to 20 kHz at ± 2 dB.

We used the National Instruments PXI-1042 to acquire and store our data; this is the data acquisition system (DAQ). The sampling frequency was 204.8 kHz, so the highest usable frequency in our data is 102.4 kHz. **Figure 2-6** shows the placement of the DAQ: where the blue circle is to the side of the linear array. The microphones were connected using ¼” BNC cables leading to boxes containing an infiniband cable which each carried 8 channels to the DAQ site; an example is shown in **Figure 2-3**. In total, 32 channels were recorded and saved at the DAQ station.



Figure 2-3 Infiniband cable box with eight channels plugged in. Plastic wrap is used to protect the connections from water and dirt. The experiment had four of these placed throughout the field.

For the pretest there were three infrasound sensors and one seismic sensor in use. These sensors were setup and maintained by Sean Maher, graduate student studying under Dr. Robin Matoza at the University of California in Santa Barbara. The sampling frequency for both sensors was 400 Hz. The Infrasound sensors were 9 Chaparral C60V. The seismometer was a 7 Trillium Compact

Posthole 120-s instrument. They were paired with DiGOS DATACUBE dataloggers. These data were used to study the coupling between the acoustic and seismic waves.

Weather needs to be documented when performing acoustic experiments. To measure the weather conditions around the testing site, I used three Kestrel model 5500L weather meters. The Kestrels were placed in a line near the mic stations at 38 m, 100 m, and 160 m. At the 38 m station, the Kestrel was placed 2.44 m above the ground; at the 100m and 160 m stations, the kestrel was placed at 3.66 m above ground. The Kestrels took data every 10 seconds for the entirety of two days. To extract the needed weather data, the time of each explosion was recorded and then the corresponding time was found in the weather data. An average of the measured temperature at the time of each explosion was taken using 30 seconds before and 30 seconds after each blast time.

2.1.2.2 Layout

The layout of this experiment consisted of four craters, a circle and then semicircle of microphone stations, and a linear array of microphone stations.

Each microphone station in the circle or semi-circle had ¼” microphones. The base the station was a tripod to which we attached wooden dowels extending out away from the tripod. The microphones were attached to the ends on the dowels via zip ties and electrical tape to minimize reflections off the stands. The microphones were first placed equidistant around 20 m radius circle at a single height. This circular array was sequentially centered on each of the four craters. Balloons were exploded in the middle of the circular array; and then the array was moved to the next location, as shown as yellow circles in **Figure 2-6**. Then, microphones were placed at two

heights, 1.22 m and 2.44 m, around the semi-circle (the right half of the large red circle in **Figure 2-6**) The semicircle, with a radius of 38 m, was centered in the middle of the four craters.

The microphone stations on the linear array (blue and red line extending out from the craters in **Figure 2-6**) were set-up with the dowels in the same way but at different heights. There was an inverted ground microphone, with the grid cap less than 1 cm off the ground; an example is shown in **Figure 2-5**. In addition, three microphones pointed skyward at heights of 1.22 m, 2.44 m, and 3.66 m at each station. These stations were approximately 100 m, 130 m, and 150 m from the center of the line of craters. The infrasound sensors were placed about 0.5 m in the ground at 100 m, 130 m, and 160 m away from the blast. The one seismic sensor was placed 1m underground at the 130 m mark.

There were two microphone stations (but just one ground microphone) approximately 100 m away from the blast, one -3.0 m in the x direction away from the ground microphone (using **Figure 2-6** as a reference for the axes), and the other -4.3 in the x direction and +1.2 m in the y direction. I still refer to these as 100 m stations because they are approximately 100 m from the craters.

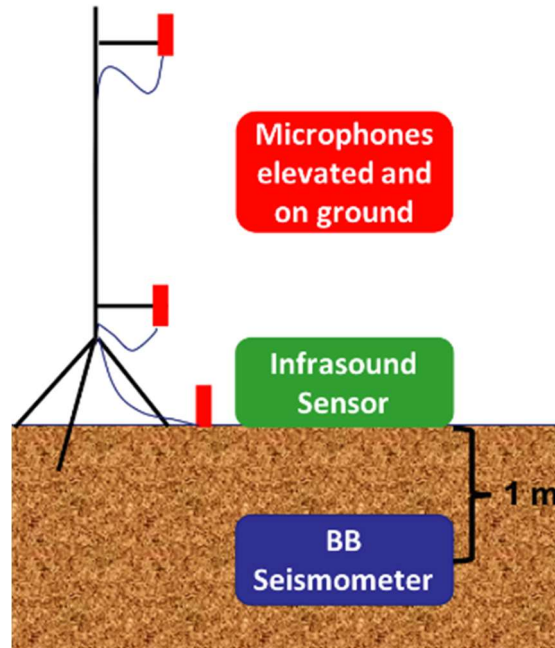


Figure 2-4 A general diagram of the set-up of a microphone station. The red boxes represent the microphone placements, the green box marks infrasound sensor placement and, 1m down underground, the blue box marks the seismometer placement. This is not an exact diagram but it useful to show the station set-up.



Figure 2-5 Picture of the "Ground Mic". All ground microphones were inverted on these three-pronged stands. The microphone is facing downwards with grid cap less than <math><1\text{ cm}</math> above the ground.

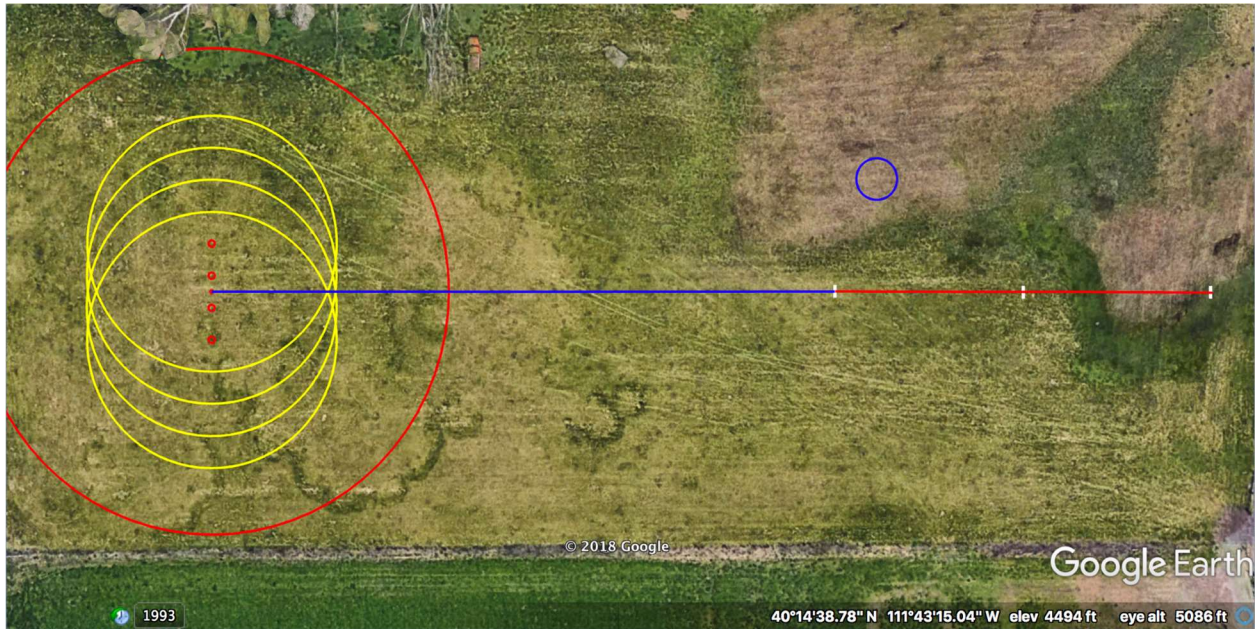


Figure 2-6 Aerial view of the Exploding Balloons set-up.

The small red circles are where each crater was placed. The yellow circles are the circles where the $\frac{1}{4}$ " microphones were placed. The large red circle was where the semi-circle microphones were placed for the second half of tests. The white tic marks on the line are the placements of the array stations. The small blue circle off to the side is where the DAQ site was.

2.1.2.3 Procedure

While conducting the experiment, there were two teams, one by the DAQ station and another down about 40 m away from the blast sites. The teams communicated by walkie talkie and phone calls. The team closer to the craters prepared the balloons and the ignition. A model rocket ignitor commonly used with fireworks was placed against the balloon in the craters. The DAQ team signaled when they started recording and the countdown to ignition began. Since the explosions were high amplitudes, everyone had ear coverings or ear plugs for safety. A few seconds after each blast, we stopped the DAQ to ensure the full waveforms would be recorded at

the farthest microphone. This procedure was repeated many times with balloons of different sizes.

2.2 Geohazards Workshop Test

2.2.1 Background

The University of Buffalo's Center for Geohazards Studies hosted and coordinated an NSF-funded, open workshop on July 26th, 2018, which is referred to as the Geohazards workshop.

Three main groups of people attended, with our group being part of the real-time measurements group to measured acoustical data during the actual explosions. The other two groups were post-blast data collection groups, one proximal or close to the blast, and one distal or any measurement taken more than 20 m away from the blast. The experiments from these other groups included studying the debris scattered from the explosions and the morphology of the ground before and after the explosions².

2.2.2 Experiment

While the pretest was designed to be as similar as possible, there are still significant differences between the pretest and the Geohazards Workshop. The recording and DAQ equipment were the same as used in the pretest (see Section 2.1.2.1). The differences between the experiments are in the source of the blasts and changes to the overall layout. The basic layout was similar, with a semi-circle and an array, but the number of microphones and their placements differed.

2.2.2.1 Equipment

The equipment was very similar to the previous experiment. The elevated semicircular array used the ¼" microphones; the ground mic at 90 degrees on the semicircle and the line array used

the ½” microphones. The infrasound sensors and seismometers were the same makes and models used in the pretest. More specific information can be found in section 2.1.2.1.

Instead of oxyacetylene balloons as our source, this experiment used buried explosives. Each explosive charge contained 90 g of Pentex, a mixture of PETN (pentaerythritol tetranitrate) and TNT (trinitrotoluene). This mixture was found to be optimal at the depth used in a previous study at the same space in the University at Buffalo⁹. The energy of each charge is 0.437 MJ.

2.2.2.2 Layout

We set up our equipment the day before the blast. Each microphone station was generally set-up similarly to that of pretest using dowels to extend out from the tripod and the three-pronged stands for the ground microphones.

For the stations in the semicircle, the microphones were placed at heights of 1.22 m and at 2.44 m. These stations were placed 30 m from the center of the four blast pads. There were seven stations placed in the arc. The stations start at 0° to 180°, with the 90° station being the start of the linear array seen in **Figure 2-7**. This station at 90° also had a ground microphone, an infrasound sensor, and a seismometer, so we could include it as a point in the array.

The line array was longer in the Geohazards workshop. There were seven microphone stations at distances from 30 m to 330 m placed every 50 m. Each station had two microphones: a ground microphone facing downwards towards the ground and a microphone 4 m above the ground.

These stations also had an infrasound sensor just below the ground and a seismometer 1 m deep into the ground.



Figure 2-7 Aerial view of the set-up at the University of Buffalo Geohazards Workshop. The blast pads are marked with yellow. The array line extends out from the center of the blast pads to the last station. The array stations are marked with red circles which are placed 30 m, 80 m, 130 m, 180 m, 230 m, 280 m, and 330 m from the blast pads.

There were four different blast pads used as the sites of the buried explosives placed 4-5 m apart. Each pad contained three charges buried between 30-35 cm below the surface and three more charges buried 60-70 cm below the surface and directly below the first set of charges. The layouts of these charges can be seen in **Figure 2-8** showing both the aerial view and the side view of the four pads. Each blast has a sequence of six charges that detonate 0.5 sec apart. The order of the charges detonated changed with each pad.

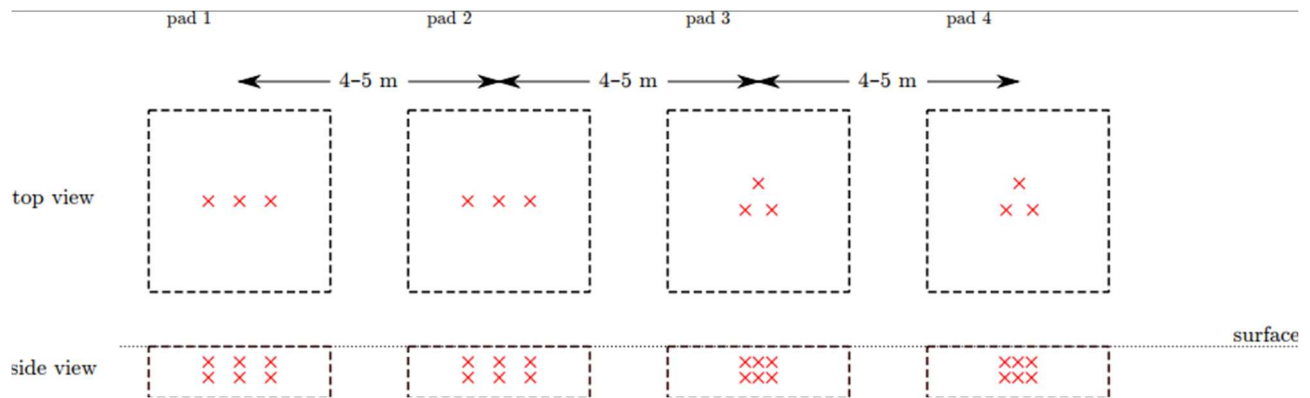


Figure 2-8 Layout of the dynamite in the ground for each blast pad.

The red x's mark the placements of the charges. The top row shows the aerial view of the explosives' placement, and the bottom row shows the side view looking at the explosives' placement straight on underground. On the bottom row the surface of the ground is marked with the finely dotted line.

2.2.2.3 Procedure

In this experiment there were three phases to each blast. A preparation phase, the blast phase, and a post-blast data collection phase. In the preparation phase, the experimenters set up the equipment to measure the blast; this time was used to test our equipment. In the blast phase, the real time recording group starts recording, the countdown is initiated, and the blasts detonate. Our research team, started recording with the countdown, recorded through the blast, and then stopped recording a few seconds after the blast. In the post-blast phase, additional data was collected. For example, the ejecta group marked where colored ping pong balls (originally buried among the explosives) landed as a result of the blasts. Our team also used this time to plot the waveforms (very simple plots) on all the microphones to check for any equipment malfunctions.

3 Results and Conclusions

3.1 Analysis Methods

The recordings were manually started, which means that each file has a different amount of time before each blast goes off. To account for this, I needed to time align the data. When recording acoustic data, pressing start causes all the microphones in the entire set-up to start recording at the same time. Therefore, the individual microphones did not need to be independently aligned, I only needed to align the different recording times with each other. I found the initial blast time for the closest and most direct microphone (the lowest microphone at the 90 degree position). Then I subtracted 0.0625 seconds from the blast peak and selected that sample number to be the starting sample. I then applied that starting sample number to the remaining channels.

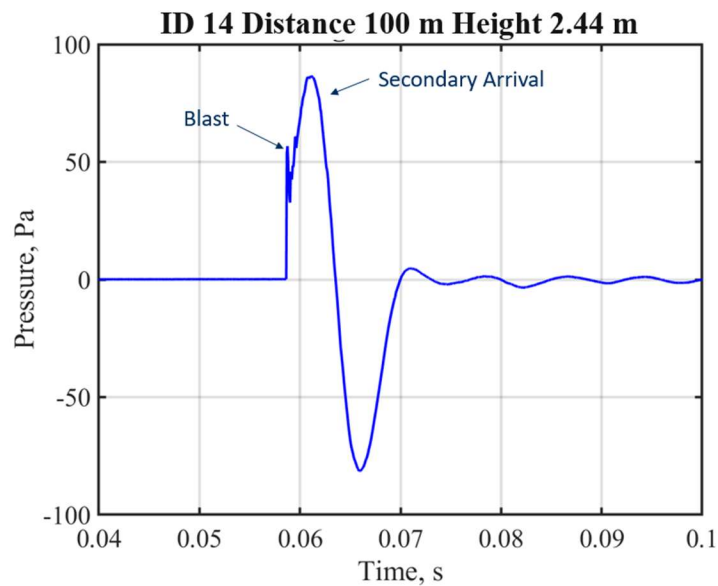


Figure 3-1 Example waveform from the Exploding Balloons Pretest.

This specific microphone was 100 m away from the blast and 2.44 m above the ground. The first spike in amplitude is what we referred to as the blast wave and the second lower frequency wave is referred to as the secondary arrival.

I also needed to extract the amplitudes of the peaks of each blast. As seen in **Figure 3-1**, there are two peaks we are identifying, the blast peak and the secondary peak. Because I want to find two local maximums, I cannot use a simple maximum function. Using MATLAB, I first found the point in the wave where the sound exceeds 10 Pa. From that point in time to 0.5 ms later, I found the maximum. From analyzing each waveform, I found no blast section of the wave lasts longer than 0.5 ms, so that was used as a safe window to find the blast peak. To find the secondary peak, I identified the window starting from the end of the previous window to the end of the recording. Finding the maximum in that window provided the secondary peak. Once I found the peak points, I recorded the location in the time aligned sample, the amplitude of the peak, the channel number, and the ID number.

The specific ground wave in these signals is a trapped surface wave. Embleton provides a defining features of a trapped surface wave: “with increasing distance from the source, the decrease in sound-pressure level due to this energy loss eventually exceeds that due to geometrical spreading and the surface wave decreases rapidly⁴.” Thus, the decrease in amplitude needs to be more pronounced than just the decrease in amplitude we expect to see with spherical spreading. The existence of a ground wave can also be proven if the amplitude of the secondary arrival wave decays as height increases⁴.

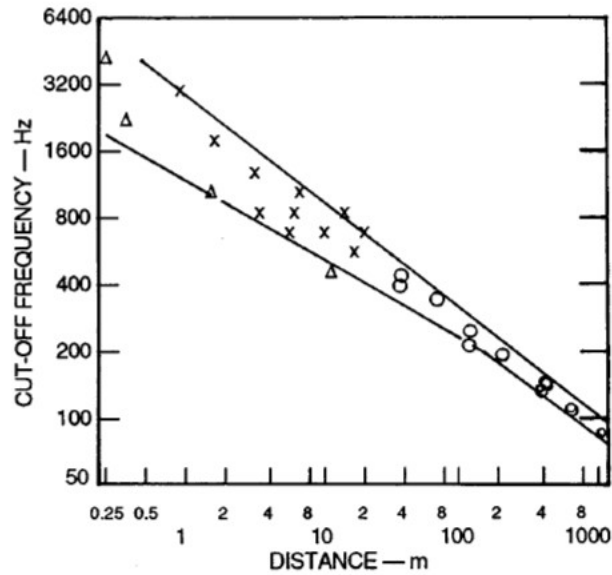


Figure 3-2 Cutoff frequency of ground wave based on distance from source. This figure is from the Embleton 1996 tutorial⁴, which is referenced throughout this paper. The three different symbols are from three different tests compiled together to create this chart. At a distance, the cutoff frequency of the ground wave is between the two lines created from analyzing the symbols.

The last way to prove the existence of the groundwave discussed in this thesis is the cutoff frequency after the initial blast wave. The projected cut-off frequencies we should see are shown in **Figure 3-2** as a function of distance from the source. If the secondary arrival wave is a ground wave, then the frequency content of the signal should cut off in the range marked in **Figure 3-2**⁴. These criteria are used to identify the secondary arrival in the acoustic signals as a trapped surface wave.

3.2 Exploding Balloon Results

The acoustic signals from the exploding balloons in the pretest showed a clear secondary arrival wave. An example of the waveform and spectrogram are shown in **Figure 3-1** for a microphone

at a height of 1.2 m and a distance 100 m from the source (a balloon placed on the ground). The large low frequency wave that appears right after the blast peak in was a clear sign of another wave existing aside from the direct sound wave from the blast. Since our sources were on the ground, this was not a reflected wave that is often present in acoustic data from elevated blast sources.

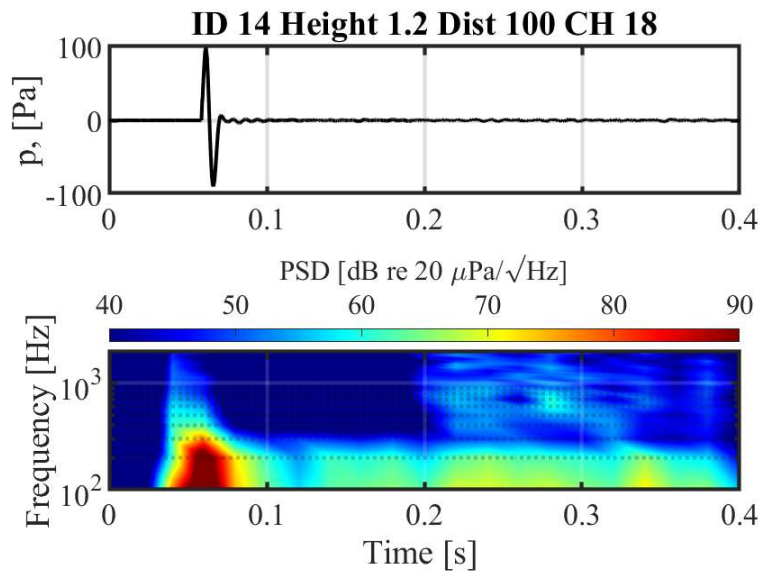


Figure 3-3 Waveform and Spectrogram of the microphone 100 m from the source and 1.2 m above the ground from the exploding balloons test. The waveform and spectrogram are of the same signal so they are approximately time aligned.

By plotting the spectrograms of each waveform, I was able to see the cutoff frequencies expected of a ground wave. The spectrogram in **Figure 3-3** clearly illustrates a cutoff in the PSD at around 300 Hz. This lines up with the expected cutoff frequency from the Embleton tutorial⁴ (**Figure 3-2**) at the 100 m distance, where the expected cutoff is between 200 and 400 Hz. This observation was true for all microphones at this station (varying heights). This pattern is also evident at 130 m and at 160 m.

The secondary arrival wave in the Pre-Test showed a clear decay over height for all the signals. This decay is true for every recording station. The decay can be seen by plotting the peak amplitude of the waves as a function of height. An example is given in **Figure 3-4** for one of the blasts recorded on microphones at four different heights at a distance of 130 m from the source. A line of best fit over height is applied for every station. For the 100 m station, the line of best fit had an R^2 value of 0.7891, for the 130 m station the R^2 value was 0.9462, and for the 160 m station the R^2 value was 0.9746. These R^2 values show a very high confidence of the linearity of this decay. While the station at 30 m did show a decay with height, I could not apply a line of best fit since there are only two heights and that would only give us two points.

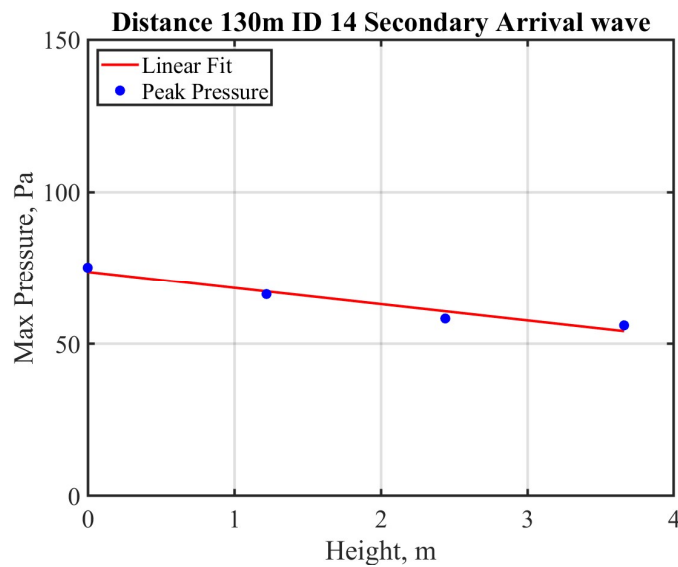


Figure 3-4 Plot of the peak pressures of the Secondary Arrival wave as a function of their height. The peak points are shown in blue, and the linear line of best fit is shown in red. These are from the microphone station 130 m away from the blasts.

In addition to the cutoff frequency and the amplitude decay with height, decay with distance should be greater than geometric spreading for a trapped surface wave. A similar process is applied to the peaks, but now data from microphones with the same height are plotted as a

function of distance. An example is shown in **Figure 3-5**: the blue dots indicate the measured peak level of the secondary arrival, and the red line shows an exponential fit to the data. The amplitude of the secondary arrival decays faster than what is expected from cylindrical spreading (black line). This pattern is seen in signals at all heights. The exploding balloons do show a decay with distance, but a key analysis is to see if this decay is greater than geometric spreading. The cutoff frequency and amplitude decay with height and over range of the secondary arrival match the three characteristics that Embleton identified for a trapped surface wave. The cutoff frequencies shown in **Figure 3-3** are those we expect to see from a trapped surface wave (explained in **Figure 3-2**). We also see a significant decay of the waves with height. The decay of the secondary arrival is a lot faster than the decay we expect to see from geometric spreading. According to Embleton, these three pieces of evidence point towards our secondary arrival being a ground wave, specifically a trapped surface wave⁴.

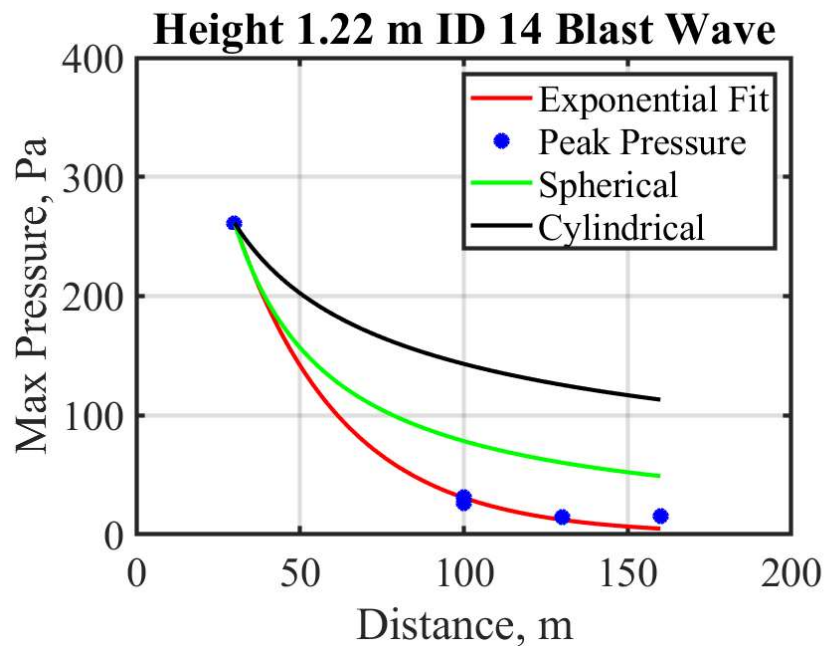


Figure 3-5 Peak amplitudes of the secondary arrivals in the waveforms compared to geometric spreading as a function of distance.

The blue points are the measured values of the peak of the secondary arrival wave at a distance of 30 m, 100 m, 130 m, and 160 m away from the blast source. All the microphones were at a height of 2.44 m above the ground. The red line is an estimated exponential line of best fit from the blue points. The green line is the expected decay due to spherical spreading, and the black line is the expected decay from cylindrical spreading.

3.3 Geohazards Workshop

The acoustic signals from the Geohazards Workshop were messier than the pretest; the biggest concern being a less consistent appearance of a secondary arrival wave. Our preliminary analysis found several things that could have caused this. The amplitude of the acoustic show waves from the buried Pentex blasts were significantly lower than in the exploding balloons test; this lower amplitude means a secondary wave would have a lower amplitude. Another contributing factor to a lack of evidence of a secondary arrival could be the ground itself. The pretest was conducted in a plowed grazing field; the ground was soft and approximately flat, making it easier for an acoustic wave to travel through. At the Geoacoustic Workshop site, the ground was rocky and dense. The ground qualities were learned in both experiments' holes were dug to bury a seismic dampening box⁸, infrasound sensors, and seismic sensors. Our final problematic variable was the explosions were also at the bottom of a small hill. The semicircular array was based on ground level with the blasts, but the line array was about a meter higher. This rise likely means that at least some of the acoustic waves traveling in and along the porous ground may have been absorbed before reaching some of our microphones.

An example of the acoustic signals recorded as a function of distance along the line array are shown in **Figure 3-6** Time aligned, normalized waveforms for "Pad 4" (in **Figure 2-8**) from the ground microphones at all distances.

The microphones were placed within 10 cm of the ground at the location in **Figure 2-7**. The acoustic signals, from microphones placed within $< 1\text{cm}$ of the ground, are shown for “Pad 4” (See **Figure 2-8**). These waveforms are time aligned and normalized by the largest value at each distance to make them visible.

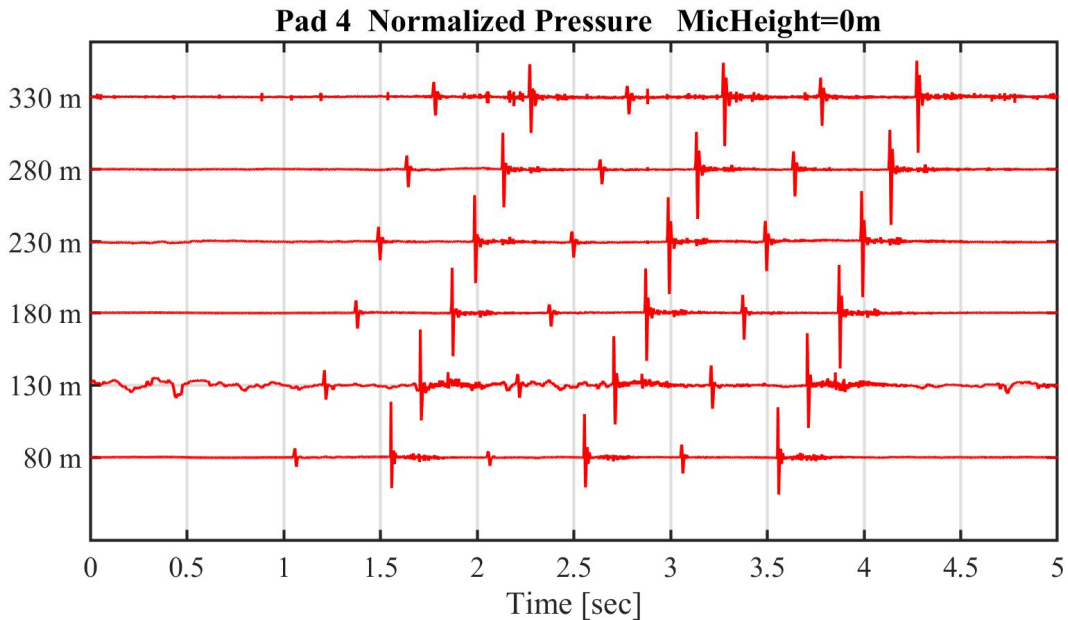


Figure 3-6 Time aligned, normalized waveforms for “Pad 4” (in **Figure 2-8**) from the ground microphones at all distances.

The microphones were placed within 10 cm of the ground at the location in **Figure 2-7**.

I conducted the same analyses to search for evidence of a secondary arrival from each of the six blasts. First, the same spectrogram analysis was applied on the data from this experiment. An example of this is shown in **Figure 3-7**. In comparing our spectrograms to **Figure 3-2**, the cutoff frequencies match up to the cutoff in our spectrograms: expected cutoff frequency for a microphone 230 m away should be between 150 and 230 Hz. The spectrograms appear to have amplitudes die out significantly above that range of frequencies, especially after the initial blast.

However, the time and frequency resolution in the fast Fourier transform make it difficult to make a definitive statement.

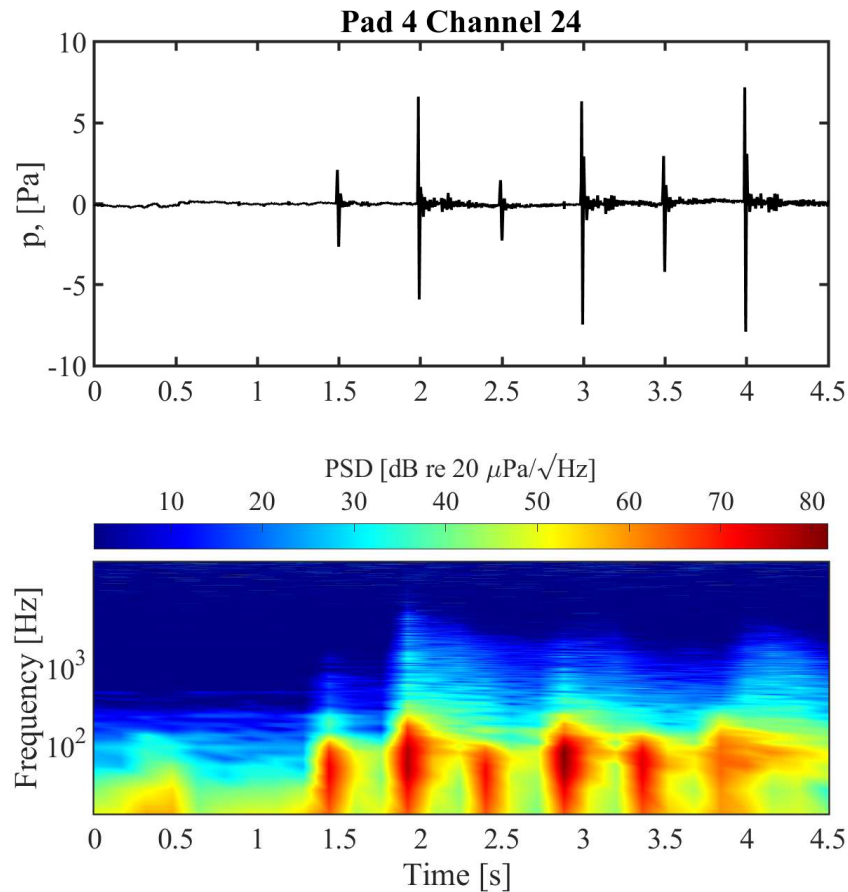


Figure 3-7 The waveform and spectrogram for the ground microphone a distance of 230 m from the source.

The second analysis to find if a ground wave exists is that the peak amplitudes of the secondary arrival need to decay as distance increases faster than geometric spreading. An example of this is seen in **Figure 3-8**, which shows the decay of the ground microphones from the first blast of “Pad 2.” This pattern is seen in all the blasts and at every height.

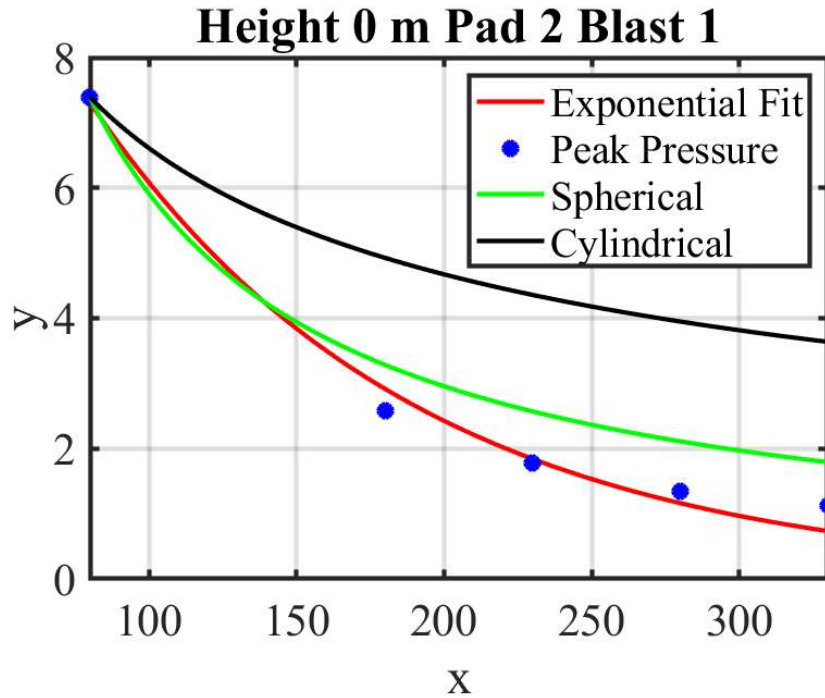


Figure 3-8 Peak amplitudes of the secondary arrival compared to geometric spreading as a function of distance.

The blue points are the measured values of the peak of the first blast wave at a distance of 80 m, 180 m, 230 m, 280 m, and 330 m away from the blast source. All the microphones were at a height of < 1 cm above the ground. The red line is an estimated exponential line of best fit from the blue points. The green line is the expected decay due to spherical spreading and the black line is the expected decay from cylindrical spreading.

The cutoff frequency and the rapid decay of the secondary arrival peak amplitude both imply the potential existence of a ground wave in this experiment. These two phenomena are present in every clear signal we have in our data.

3.4 Conclusion

This thesis compares blast waves from oxyacetylene balloons from the exploding balloons test and buried explosives from the Geohazards workshop. The exploding balloons test took place in a plowed field in Provo, Utah using oxyacetylene filled balloons as the blast source. The

Geohazards Workshop took place in a special site near the University of Buffalo, New York and used buried explosives as the blast source. More details about these experiments can be found in Chapter 2, but key difference between the two are the ground type and blast source.

My research focused on determining if the secondary arrival is a trapped surface wave, as defined by Embleton in his “Tutorial on Outdoor Sound”⁴. The exploding oxyacetylene balloons show a clear secondary arrival wave to appear. This secondary arrival has the same characteristics as a trapped surface wave: 1) the cutoff frequencies we see in the spectrograms (e.g., **Figure 3-3**), 2) amplitude decay over height (e.g., **Figure 3-4**), and 3) amplitude decay over distance that exceeds the decay caused by spherical spreading(e.g., **Figure 3-5**).

The buried explosives at the Geohazards workshop show preliminary evidence of a ground wave based on the cutoff frequencies in the spectrograms and the decay exceeding that caused by spherical spreading. The acoustic waves had lower amplitudes than the balloons, the terrain contained a hill, and there was a large bush/tree that all contributed to difficulty in analyzing the data, so no firm conclusions have yet been reached.

A lot of potential analyses remain. Further research will include closer analysis of the Geohazards Workshop decay rate and a proper accounting for the environmental variables. In addition, the difference in wave amplitudes should be analyzed based on the shapes of the different craters in the pretest (**Figure 1-2**) and based on the placement and order of detonation of the buried explosives in the Geohazards Workshop (**Figure 2-8**).

Appendix A

Computer Codes

This section is to document the codes used in this thesis and what figures they made to keep the repository organized.

Code	Use
ReadinMicDataAlignPads.m	Time aligns microphones
PlotMicArraySpecgram.m	Used to make Figure 3-3 , plots both waveform and spectrogram
PlotPeaksHeight.m	Used to make Figure 3-4 , plots the peaks from the Exploding Balloons at the same distance with varying heights
PlotPeaksDist.m	Used to make Figure 3-5 , plots the peaks from the Exploding Balloons at the same height with varying distance
PlotMicDataDist.m	Used to make Figure 3-6 , plots the normalized waveforms from the Geohazards Workshop at one height in every distance stacked on one chart
PlotMicWaveformSpectra.m	Used to make Figure 3-7 , plots the waveform and the spectrogram on top of each other
BuffaloExtractPeaks.m	Used to extract the peak pressures from each blast in each waveform for the Geohazards Workshop
BuffaloPlotPeaks.m	Used to make Figure 3-8 , plots the peaks from the Geohazards Workshop at the same height with varying distance

Specific Data Information

The nature of field experiments, especially outdoor acoustic experiments, means that not all the data we receive is perfect. Specifically, at the Geohazards Workshop we had some microphones

that didn't record the blasts correctly. We chose to throw out recordings if the acoustic signal recorded didn't exceed what appears to be electrical noise. You can see an example of this in **Figure 9** where we threw out the recording of the ground microphone at 130 m since it appears to have only recorded electrical noise.

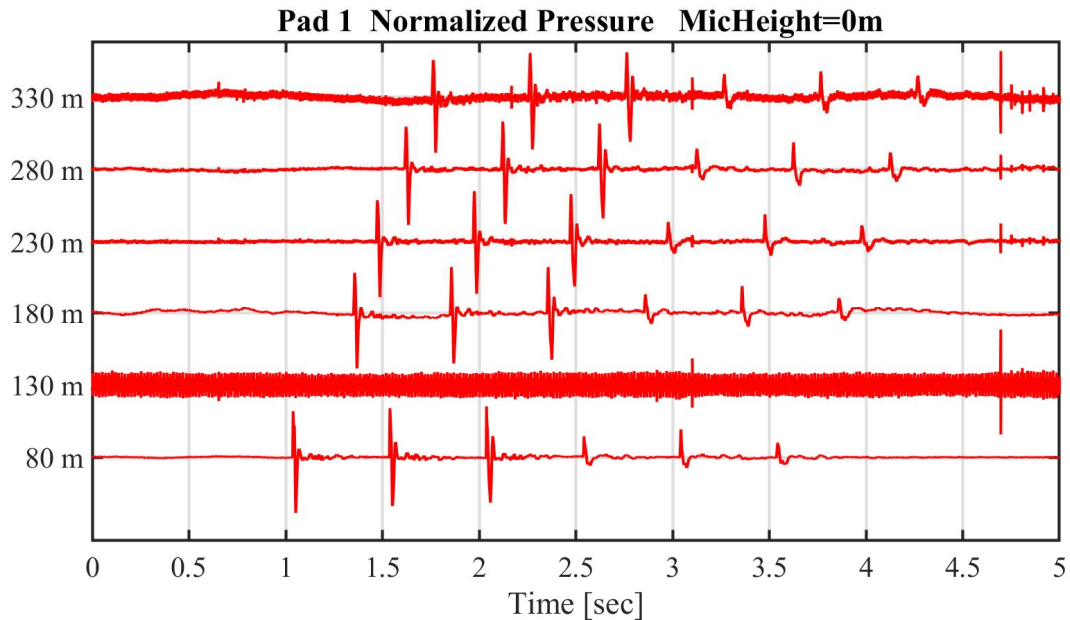


Figure 9 Normalized waveforms of the ground microphones during Pad 1 in the Geohazards Workshop stacked in order of distance. We chose to throw out the recording at 130 m (channel 18) for this set of blasts because it appears to have not recorded the acoustic signal and just recorded the electric signal.

The channels we chose to throw out for Pad 1 are channels 18, 21, 22, 27, and 29. The channels we chose to throw out of Pad 3 are channels 21, 25, and 29. Pad 2 and Pad 4 didn't have any recordings bad enough that we threw them out. In the codes for the plots used in this thesis, they are written to skip over these channels, so they run smoothly.

Weather Data – Kestrel

We took weather data to prepare for possible interference with our acoustic signals. The first table is the weather data for the Exploding Balloons experiment and the second table is the weather data for the Geohazards Workshop. The values in the table are averages over the readings at the different distances.

Time	Crater	ID#	Temp (°C)	Humidity (%)	Pressure (mb)	Windspeed (m/s)
9:43 AM	N	1	30.77	40.60	865.00	1.19
9:46 AM	N	2	29.36	39.57	864.99	1.09
10:38 AM	NC	3	30.57	36.74	864.76	1.94
11:03 AM	NC	4	31.54	33.11	864.90	2.39
1:18 PM	SC	5	32.34	36.51	863.70	2.63
1:28 PM	SC	6	32.21	33.14	863.50	2.49
2:07 PM	S	8	34.17	34.63	862.73	1.77
2:14 PM	S	9	34.07	31.77	862.70	1.36
6:31 PM	S	10	28.94	42.33	861.50	1.07
6:32 PM	SC	11	29.04	41.29	861.50	1.21
6:43 PM	NC	12	27.84	50.73	861.50	1.09
6:44 PM	N	13	27.91	49.86	861.50	1.23
7:50 PM	S	14	26.76	54.06	861.93	1.07
7:52 PM	SC	15	26.89	54.91	861.93	0.96
7:55 PM	NC	16	27.09	55.06	861.89	0.76

7:55 PM	N	17	27.09	55.06	861.89	0.76
7:59 PM	center (ground)	18	27.27	50.37	861.76	1.81
8:03 PM	center (ground)	19	27.00	51.30	861.79	1.66

Time	Crater	ID#	Temp (°C)	Humidity (%)	Pressure (mb)	Windspeed (m/s)
9:43 AM	N	1	30.77	40.60	865.00	1.19
9:46 AM	N	2	29.36	39.57	864.99	1.09
10:38 AM	NC	3	30.57	36.74	864.76	1.94
11:03 AM	NC	4	31.54	33.11	864.90	2.39
1:18 PM	SC	5	32.34	36.51	863.70	2.63
1:28 PM	SC	6	32.21	33.14	863.50	2.49
2:07 PM	S	8	34.17	34.63	862.73	1.77
2:14 PM	S	9	34.07	31.77	862.70	1.36
6:31 PM	S	10	28.94	42.33	861.50	1.07
6:32 PM	SC	11	29.04	41.29	861.50	1.21
6:43 PM	NC	12	27.84	50.73	861.50	1.09
6:44 PM	N	13	27.91	49.86	861.50	1.23
7:50 PM	S	14	26.76	54.06	861.93	1.07
7:52 PM	SC	15	26.89	54.91	861.93	0.96
7:55 PM	NC	16	27.09	55.06	861.89	0.76
7:55 PM	N	17	27.09	55.06	861.89	0.76
7:59 PM	center (ground)	18	27.27	50.37	861.76	1.81

8:03 PM	center (ground)	19	27.00	51.30	861.79	1.66
------------	--------------------	----	-------	-------	--------	------

Time	Pad #	Temp (°C)	Humidity (%)	Pressure (mb)	Windspeed (m/s)
9:55 AM	1	22.3	76.3	966	1.7
11:23 AM	2	25.2	63.7	966	2
1:50 PM	3	26.9	54.1	965	1.6
3:31 PM	4	27.1	49.3	965	2.5

Index

B

buried explosives · 3, 17

C

cutoff frequency · 22

D

direct wave

 direct sound wave, direct path · 3

E

elevated source · 4

G

ground wave

 trapped surface wave · 22

I

Infrasound · 11

O

oxyacetylene balloons

 Oxyacetylene balloons, oxyacetylene Balloons,

 Oxyacetylene Balloons, oxyacetylene · 5, 17

Oxyacetylene balloons · 30

S

scaled explosions · 2

secondary arrival wave

 secondary arrival, secondary wave · 7, 22

seismic

 seismic waves · 2, 11, 12, 13

shock waves

 shock wave, blast wave · 2, 8, 9

spectrogram · 23, 28

Spectrogram · 23

References

- ¹ Robin S Matoza , “The Inaudible Rumble of Volcanic Eruptions,” *Acoustics Today*. Vol. **14**, 17-25, Spring 2018
- ² J. Teddeucci, G. A. Valentine, I. Sonder, J. D. L. White, P.-S Ross, and P. Scarlato, “The effect of pre-existing craters on the initial development of explosive volcanic eruptions: An experimental investigation,” *Geophysical Research Letters*. **40**, 507-510 (2013).
- ³ Young *et al.*, “Outdoor measurements of spherical acoustic shock decay,” *J. Acoust. Soc. Am.* **138**, EL305-310(2015)
- ⁴ Embleton,” Tutorial on sound propagation outdoors,” *Acoust. Soc. Am.* **100** (1), July 1996
- ⁵ Leete *et al.*, “Mach stem formation in outdoor measurements of acoustic shocks,” *Acoust. Soc. Am* **138**, EL522-527(2015)
- ⁶ Escobedo, “Measuring Directionality of Acoustic Shocks from Small Scale Explosions,” University of Utah College of Physics and Astronomy, December 2018
- ⁷ Ostergaard, “Acoustic Directionality of Explosions as Scale-Model Volcanoes,” Brigham Young University College of Physical and Mathematical Sciences, December 2020
- ⁸ E. J. Lysenko *et al.*, “A prototype soundproof box for isolating ground-air seismo-acoustic signals,” *Proceedings of Meetings on Acoustics*, Vol. **36**, 045002 (2019)